THE ASTROPHYSICAL JOURNAL, 340:443–454, 1989 May 1

HIGH-ENERGY GAMMA-RAY ABSORPTION IN RELATIVISTIC MAGNETOSPHERES

H. RIFFERT
JILA, University of Colorado
AND
P. MÉSZÁROS AND Z. BAGOLY[1]
Pennslyvania State University
Received 1988 July 11; accepted 1988 October 17

ABSTRACT

We calculate the propagation of γ-rays around neutron stars with a dipole magnetic field, including the effects of general relativity and the absorption by the one-photon magnetic pair production process, as a model for the high-energy transport in gamma-ray burst sources and pulsars. We discuss the escaping photon beam characteristics as seen by distant observers at different angles with respect to the magnetic axis, for radiation arising from the polar caps of neutron stars of varying degrees of compactness and surface field strengths. The observed beaming depends strongly on the surface field only up to $B \approx 0.05$ times the critical field value, being essentially constant above the value 0.1. The gravitational light bending contributes significantly to broaden the beam profiles especially at low energies above threshold, being sensitive to the stellar radius to mass ratio.

Subject headings: gamma rays: general — pulsars — radiative transfer — relativity — stars: atmospheres — stars: neutron

I. INTRODUCTION

The process of gamma-ray propagation in relativistic magnetospheres is of relevance for models of bursting gamma-ray sources, as well as for rotation-powered pulsars such as the Crab and Vela pulsars, which are observed at energies including the range 0.3–100 MeV. The presence of hard ($E \gtrsim 10$ MeV) radiation in a large fraction of the gamma-ray bursters (GRBs) detected by the *SMM* spacecraft (Matz *et al.* 1985) provides an important constraint on the models of these objects which are based on a magnetized neutron star origin. This is because absorption by one-photon pair creation in the strong magnetic field can suppress radiation above a threshold $E \gtrsim 1$ MeV, depending on the angle between the photon wave vector and the local magnetic field direction. Monte Carlo simulations in the weak gravity limit indicate that for increasingly strong magnetic fields the escaping high-energy photons would be concentrated on a narrow beam along the magnetic axis, which would act as a strong observational antiselection effect. This has led to estimates of a typical surface field strength of $B \lesssim 4 \times 10^{11}$–$10^{12}$ G (e.g., Matz *et al.* 1985), in order to explain the *SMM* observational statistics. This is about one order of magnitude less than the measured magnetic fields in accreting pulsars, or than the values inferred for young rotation-powered pulsars. A low field is acceptable in principle, but to make this compatible with the report by Mazets *et al.* (1981) of cyclotron lines in the 20–60 keV range in a number of GRBs (implying $B \approx 4$–6×10^{12} G may require two-component or more involved models (Lamb 1988; Brainerd 1989; Zdziarski 1987). The importance of settling this point is made more urgent by the recent report (Murakami *et al.* 1988) of two GRB events detected with *Ginga* showing absorption features at 20 and 40 keV which are also most easily interpreted as cyclotron first and second harmonics. Given the controversy concerning the association of GRBs with neutron stars and the strength of their magnetic field, it is important to reexamine in greater physical detail the dependence of the escaping γ-ray flux on the various processes and on the physical characteristics of the star.

Most discussions of high-energy photon propagation and absorption in a neutron star magnetic field have been either qualitative or simplified, due to the complication of dealing with a process depending on the relative angle of propagation and the field strength, both of which vary in space. Detailed transport calculations have not been performed so far, previous results having been based on mean free path considerations or on Monte Carlo simulations involving single photons at a time. The validity of the asymptotic absorption cross section which is generally used needs to be considered at arbitrary photon energies and field strengths. More importantly, one needs to take into account the effects of general relativity on the field configuration, and the effects of gravitational bending and focusing of the photon orbits in the Schwarzschild metric of a compact neutron star. Only when the neutron star has a large radius, say $R_{\rm NS} \gtrsim 4R_{\rm S}$ [(where the Schwarzschild radius $R_{\rm S} = 2GM/c^2 = 4.2Km(M/1.4\ M_\odot)$] can one neglect this effect in an approximate treatment. For smaller radii, the gravitational light bending is expected to be strong enough to broaden appreciably the beam of escaping high-energy photons, and any estimate of the GRB detectability based on beam sizes must take this effect into account.

II. MAGNETIC ABSORPTION IN SCHWARZSCHILD SPACETIME

The mean absorption length $\kappa_A(\lambda)$ for a photon moving at an angle λ with respect to the magnetic field direction has been calculated in detail by Tsai and Erber (1974). The threshold for this process is at

$$\frac{\hbar\omega}{m_e c^2} \sin\lambda \geq 2 \,. \tag{1}$$

[1] Also Eötvös University, Budapest.

They also calculated simpler asymptotic expressions, valid well above threshold, which were improved upon by Daugherty and Harding (1986). Defining

$$\chi = \omega'(B'/2)\sin\lambda\,, \tag{2a}$$

$$\omega' = \frac{\hbar\omega}{m_e c^2}\,, \qquad B' = \frac{B}{B_c}\,, \tag{2b}$$

where $B_c = m_e^2 c^3/\hbar e = 4.414 \times 10^{13}$ G is the critical field, the asymptotic expressions are

$$\kappa_A(\lambda) = 0.23\,\frac{\alpha_f}{\lambda\!\!\!^{-}_c}\,B'\sin\lambda\exp\left\{-\frac{[1+0.42(\omega'\sin\lambda)^{-2.7}B'^{-0.0038}]}{(3/4)\chi}\right\}, \qquad \text{for } \chi \ll 1\,, \tag{3a}$$

and

$$\kappa_A(\lambda) = 0.38\,\frac{\alpha_f}{\lambda\!\!\!^{-}_c}\,\chi^{-1/3}\,, \qquad \text{for } \chi \gg 1\,, \tag{3b}$$

(see Daugherty and Harding 1983), where $\alpha_f = 1/137$ and $\lambda_c = 3.8616 \times 10^{-11}$ cm is the Compton wavelength. While most treatments use only equation (3a), we are here interested in a broad range of field strengths, frequencies, and angles, so that equation (3b) is also necessary. In the intermediate χ region, one can use the full form of the approximate expression from which equations (3a) and (3b) are derived, namely

$$\kappa_A(\lambda) = \frac{1}{\sqrt{3}3\pi}\,\frac{\alpha_f}{\lambda\!\!\!^{-}_c}\,\frac{1}{\omega'}\int_0^1 dv\,\frac{9-v^2}{1-v^2}K_{2/3}\left(\frac{8}{3B'\sin\lambda\omega'}\,\frac{1}{1-v^2}\right), \tag{4}$$

(see Tsai and Erber 1974). The integral (4) is too cumbersome for frequent use, so that we have fitted its values with a second-degree polynomial interpolation to join the large and small χ regimes described by equation (3),

$$\kappa_A(\lambda,\chi) = \kappa_A(\lambda,\,\chi \ll 1) \qquad 10^{-0.05[1.06(\log\chi)^2 + 1.77\log\chi + 1]}\,, \tag{5}$$

where $\kappa_A(\lambda,\,\chi \ll 1)$ is given by expression (3a). Equation (5) fits the integral (4) within the range $-1.5 < \log\chi < 3.0$ to better than a few percent accuracy. Expressions (3), (4), and (5) are valid above threshold, i.e., for $\omega'\sin\lambda \geq 2$, and $\kappa_A = 0$ for $\omega'\sin\lambda < 2$. Well above threshold they are accurate, while close to threshold they overestimate the exact opacity containing the sawtooth structure caused by the quantized Landau levels in the final electron and positron (see Daugherty and Harding 1983). Since the exact expressions are too complicated for extensive use, in this paper we shall use the asymptotic expressions, making allowances where necessary for their approximate nature.

The magnetic field is taken to be given by the multipole expressions in an exterior Schwarzschild metric (see Wasserman and Shapiro 1983). Thus, the magnetic dipole is [in terms of polar coordinates (r, Θ, Φ)]

$$B_r = \frac{2\mathcal{M}}{r^3}\cos\Theta\,\mathcal{F}_1(r)\,, \tag{6a}$$

$$B_\Theta = \frac{\mathcal{M}}{r^3}\sin\Theta\,\mathcal{F}_2(r)\,, \tag{6b}$$

where

$$\mathcal{F}_1(r) = -3r^2\left[r\ln\left(1-\frac{1}{r}\right)+1+\frac{1}{2r}\right], \tag{7a}$$

$$\mathcal{F}_2(r) = 6\,\frac{r^2}{\sqrt{1-1/r}}\left[(r-1)\ln\left(1-\frac{1}{r}\right)+1-\frac{1}{2r}\right], \tag{7b}$$

and the magnetic moment $\mathcal{M}$ can be expressed in terms of the surface magnetic field B_0 at the pole,

$$B_0 = B_r(\Theta = 0) = \frac{2\mathcal{M}}{R^3}\mathcal{F}_1(R)\,, \tag{8}$$

where R is the neutron star radius, and all radii are in Schwarzschild units. The modulus of the magnetic field at (r, Θ) is given by

$$B = \frac{\mathcal{M}}{r^3}\,[\mathcal{F}_2^2(r)\sin^2\Theta + 4\mathcal{F}_1^2(r)\cos^2\Theta]^{1/2}\,. \tag{9}$$

The polar cordinates (r, Θ, Φ) refer to the observation point, while the coordinates (μ, ϕ, ω), where $\mu = \cos^{-1}\theta$, refer to the photon

four-momentum quantities, the first two being direction and the third the photon frequency. The cosine of the angle between the photon wave vector and the magnetic field is

$$\cos\lambda = [\mathscr{F}_2^2(r)\sin^2\Theta + 4\mathscr{F}_1^2(r)\cos^2\Theta]^{-1/2}[2\mu\cos\Theta\mathscr{F}_1(r) + \sqrt{1-\mu^2}\cos\phi\sin\Theta\mathscr{F}_2(r)]\,. \tag{10}$$

at the position point (r, Θ). Thus, we have the dependence $\lambda \equiv \lambda(r, \Theta, \mu, \phi)$.

III. EMISSION AND TRANSPORT MODELS

In order to investigate the survival of the high-energy photons in a nonuniform magnetic field including general relativistic effects, it is convenient to use a simplified emission model. We shall assume that there is a source of photons of various energies, which will be taken to be at or near the stellar surface, and that these photons are depleted by the process of equations (3)–(5), giving rise to pairs. The pairs loose their perpendicular energy by synchrotron emission, and the remaining parallel energy plus the rest mass can be used to create secondary photons by annihilation. However, these secondary synchrotron and annihilation photons can be approximately neglected, as far as the transport in the 1–10 MeV region is concerned. This can be seen as follows. Consider the center of mass frame ($\boldsymbol{k}\cdot\boldsymbol{B} = 0$). From the pair production attenuation coefficient one can calculate the pair energy distribution (see Daugherty and Harding 1983), and it turns out that the most significant final states are those with almost no parallel momentum ($p \approx 0$). In addition, for $\omega' B' < 1$ the initial photon energy is shared almost equally between the positron and the electron. Then all the energy goes into Landau level excitation with

$$j \approx j_{\max} = \left[\left(\frac{\omega}{2m}\right)^2 - 1\right]\frac{B_c}{2B}$$

(we use natural units $\hbar = c = 1$ throughout). We get a typical de-excitation time scale from the synchroton loss rate (Rybicki and Lightman 1979)

$$t_s^{-1} = \frac{P_{\rm sync}}{\epsilon} = \frac{4}{9}\frac{\alpha_f}{\lambda_c}\frac{m}{\epsilon}(\gamma_{\rm L}^2 - 1)\left(\frac{B}{B_c}\right)^2,$$

where the Lorentz factor $\gamma_{\rm L}$ follows from

$$\gamma_{\rm L} = \frac{E}{m} \approx \sqrt{1 + 2j_{\max}\frac{B}{B_c}} \approx \frac{\omega}{2m}$$

(note that $\omega/m > 2$), and $\epsilon = E - m$ is the excitation energy of the pairs. From that

$$t_s \approx 3.97\times 10^{-19}\left(\frac{\omega}{2m} + 1\right)^{-1}\left(\frac{B}{B_c}\right)^2 \text{ s}\,. \tag{11}$$

This time scale, which is usually quite short, has to be compared to a typical annihilation time scale t_A. For $B/B_c > 0.2$ one-photon annihilation is the dominant process, with a time scale given by (see Daugherty and Bussard 1980)

$$t_A^{-1} = n_p\alpha_f\lambda_c^2\frac{m^2}{m^2+p^2}\frac{B_c}{B}\exp\left[-2\frac{B_c}{B}\left(1+\frac{p^2}{m^2}\right)\right],$$

where n_p is the pair density. Since $p^2 \ll m^2$ for the annihilating pairs (see above), we have

$$t_A \approx 3.06\times 10^{12}\frac{1}{n_p}\frac{B}{B_c}\exp\left(2\frac{B_c}{B}\right)\text{ s}\,,$$

and thus

$$\frac{t_s}{t_A} \approx 1.30\times 10^{-31} n_p\left(1+\frac{\omega}{2m}\right)^{-1}\left(\frac{B_c}{B}\right)^3\exp\left(-2\frac{B_c}{B}\right).$$

The function of B/B_c has its maximum value at $B/B_c = 0.667$; therefore

$$\frac{t_s}{t_A} < 1.0\times 10^{-32} n_p\left(1+\frac{\omega}{2m}\right)^{-1}. \tag{12}$$

For smaller fields ($B/B_c < 0.2$) two-photon annihilation becomes more important, and the corresponding cross section can be approximated by the free space value (Daugherty and Bussard 1980); for small pair momenta ($p^2 \ll m^2$) we have

$$t_A^{-1} = 2\pi\alpha_f^2\lambda_c^2 n_p \approx 1.50\times 10^{-14}\text{ s}^{-1}\,,$$

and thus

$$\frac{t_s}{t_A} \approx 6.0\times 10^{-33} n_p\left(1+\frac{\omega}{2m}\right)^{-1}\left(\frac{B_c}{B}\right)^2. \tag{13}$$

Typically $n_p \approx 3 \times 10^{20} L_{38} R_6^2$ cm^{-3}, and $B_c/B < 100$, so that the ratios (12) and (13) are quite small except for extremely high luminosities or low magnetic fields. In general, the γ-photons will create pairs in a high Landau level, which decay rapidly to the ground state. The energy of the synchroton photons is approximately given by

$$\omega_{\rm sync} \approx \left[E - m; \left(\frac{E}{m}\right)^2 \frac{B}{B_c} m \right], \tag{14a}$$

and they are emitted essentially perpendicular to the magnetic field (note that our considerations so far are valid in the center of mass frame). Returning to the stellar frame we have

$$\omega = \omega^* \sin \lambda , \qquad \omega_{\rm sync} \approx \omega^*_{\rm sync} \sin \lambda , \tag{14b}$$

with λ being the local angle of propagation for the primary photons respect to the magnetic field. If $\omega_{\rm sync} > 2m$, the secondary photons will be reabsorbed, making pairs which will further cool. For $B < 0.1 B_c$ and primary photons $\omega < 10$ MeV, however, a large fraction of secondaries has energies below threshold (i.e., $\omega_{\rm sync} < 2m$). In the stellar frame of reference the energy of these particular photons, which will not be absorbed by pair production, can be either above or below $2m$, depending on the propagation angle λ. In fact, from equations (14a) and (14b) it is possible to derive a range of angles such that $\omega^*_{\rm sync} > 2m$. In our transport calculations, however, we will neglect this local source of high-energy photons, because we are considering a primary emission function which is essentially isotropic, and the above range of λ-values is always less than a few percent of π.

Depending on the model of production, the initial photons might arise at some distance above the surface, but in practice this would be similar to the case of emission from a star of larger radius (this being the radius of emission), since we need only be concerned with the outward emission. This is because, unless the emission occurs very high, the downward directed photons would either be absorbed in the increasing field or be thermalized and degraded at the surface. In this type of model the emission is usually assumed to come from a small fraction of the total surface, typically around the magnetic pole. The size of the active polar caps depends on the specific mechanism of energy production or deposition. Without going into actual model details, which is not our purpose, we shall investigate the effect of varying the cap opening half-angle α. The dependence of the absorption process on the stellar radius, or strength of the surface gravity, needs to be considered in some detail, since it affects the relative escape probability of photons emitted at different energies and in different directions. In addition, one must consider also the variations in the absorptivity as a function of the magnetic field strength radius. However, since the absorption begins and is strongest at the surface, in order to distinguish the surface gravity effects from the absorption effects we shall consider situations with a varying radius (in Schwarzschild units) and the same surface field strengths.

If we consider only photon absorption by e^+-e^- pair production in the external magnetic field of a neutron star neglecting photon emission, the transfer equation for the high-energy λ-rays reads

$$\frac{df}{ds} = -\kappa_A f . \tag{15}$$

The transport equation (15) can be expressed in terms of characteristic coordinates in a Schwarzschild metric, and cast as a differential equation dependent on a single variable τ along the curved photon path, whose integration gives a solution for the invariant photon distribution function f (see Appendix A). The solution for an observer at the distance $r_{\rm obs}$ is

$$f = f_0 e^{-\tau} , \tag{16}$$

where τ is the optical depth along the curved photon path between the surface at R and the observation point at $r_{\rm obs}$. Details of the transfer equation and the method of solution are given in Appendix A. This deceptively simple looking equation, which must be solved numerically, gives the evolution of the phase space distribution function f, which contains more information than the simple survival probability of a single photon available from Monte Carlo calculations. The quantity τ at different points along each photon orbit depends implicitly on the local coordinates and photon four-momentum quantities as well as on the initial values of these quantities. The total photon flux and the energy flux are obtained from f by multiplying with the square or the cube of the frequency, respectively, and integrating over the entire emission regime.

IV. ESCAPING PHOTON FIELD

The numerical results for the escaping photon flux depend on the surface field value and on the stellar radius in Schwarzschild units, i.e., on the strength of the surface gravity. For a relatively weak magnetic field of $B_0 = 0.01 B_c$ (i.e., $B_0 = 4.413 \times 10^{11}$ G), specified at the pole, the absorption is weak, and most photons above $\omega \gtrsim 2$ (in units of the electron rest mass) are able to escape over a range of angles determined by the curvature of the field lines and, to a varying amount, by the gravitational light bending. The escaping beam shape for this value of the field and one polar cap only with opening half-angle $\alpha = 5°$ is shown in Figure 1. For two caps, the beam can be obtained by adding the contribution of the same beam as a function of $\pi - \Theta$. For $R = 1.7$ Schwarzschild units (Fig. 1*a*), the high-energy photons ($E \gtrsim 10$ MeV) must originate with initial angles close to the field and are only able to escape within a cone of 30°–35° width about the polar axis, while in the range 4–5 MeV the escape occurs over a broad range extending to $\sim 80°$. At lower energies the photons escape over essentially the whole range of initial angles, and reach final escape angles up to π, being bent and focused in the direction of the antipodal polar cap. This causes the cusping seen in Figure 1*a* at angles near $\approx \pi$ at low energies. This cusping would appear near 0 in a two-pole configuration, due to the reflection symmetry. For a larger radius of $R = 2.5$ (see Fig. 1, *middle panel*) the $E \gtrsim 10$ MeV beam is only slightly less than 30°, and around 4–5 MeV slightly less than 80°. For $E \lesssim 3$ MeV the difference from the previous radius is more drastic, the beams no longer bend over, and them cut off at $\sim 120°$. For two poles, however, this still gives a high chance of detection. For large radii $R = 5$ (see Fig. 1*c*, *lower panel*), the $\gtrsim 10$ MeV beam is

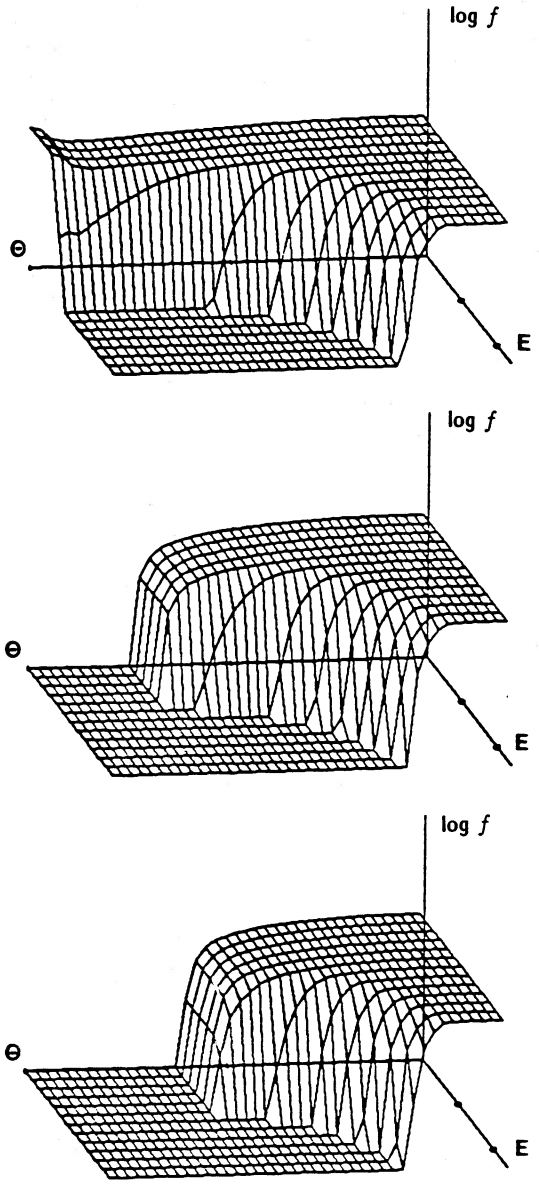

FIG. 1.—Beam shape for $B_0 = 0.01B_c$, and one polar cap of opening half-angle $\alpha = 5°$, for radii in Schwarzschild units of (*a*) $R = 1.7$ (*b*) $R = 2.5$, and (*c*) $R = 5$, plotted as a function of the energy in MeV and angle Θ at the observer. The *z*-axis gives $\log_{10} f$ between 0 and 10^{-4}, the *x*-axis in the plane of the figure is Θ between 0 and π in linear steps of 4°.5, and the *y*-axis (out of the plane of the figure) is the photon energy *E* going up to 12 MeV in linear steps of 1 MeV. These are all observer quantities. The value of the invariant photon distribution *f* at the origin of *E* and Θ is the initial, unattenuated value.

down to 25°, while at 1–3 MeV it is $\sim 90°$. While for the more relativistic configurations of $R = 1.7$ and $R = 2.5$ the beam close to 1 MeV is almost flat at all angles (except for the focusing cusp near π), for radii where the light bending is very weak, such as for $R = 5$, the 1–3 MeV beam shows a noticeable tapering between 0 and 90°.

For a stronger surface magnetic field of $B_0 = 0.05B_c$, the results are shown in Figure 2 for one polar cap of 5° opening half-angle. The effects of gravity are not able in this case to modify the stronger magnetic absoption effects significantly. In the top panel, for $R = 1.7$, the $E \gtrsim 10$ MeV beam is constrained within $\lesssim 10°$, the 4–5 MeV is less than $\sim 15°$, and at 3 MeV the beam is only $\sim 25°$–30°. It is only below ~ 1 MeV that photons are able to escape over a broad range of angles, when the absorption condition is close or below threshold. For $R = 2.5$ (see Fig. 2, *middle panel*) the beam widths at the same energies are somewhat narrower, and down to 120° for $\lesssim 1$ MeV. For $R = 5$ the beams above $\gtrsim 2$ MeV narrow down only very slightly, the magnitude of the angular beam widths not being very strongly dependent on gravity. Rather, it is the magnetic effects that dominate, and the beam shape variation is in good part due to the magnetic field line direction dependence on the field strength (eqs. [6a]–[6b]). A further increase of the surface magnetic field leads to beam shapes that remain practically the same. The beam shapes for $B_0 = 0.1B_c$ are shown in Figure 3, and qualitatively they do not differ much from those for $B_0 = 0.05B_c$. A further increase of the field does not lead to anything new, the beams for $B_0 = B_c$ being identical to those for $B_0 = 0.1B_c$. This is due to a saturation of the magnetic absorption effects, which can be understood from a qualitative discussion of the transport (see § V and Appendix B).

Another parameter which has an influence on the size of the beams is the cap size. For larger polar cap opening half-angles the

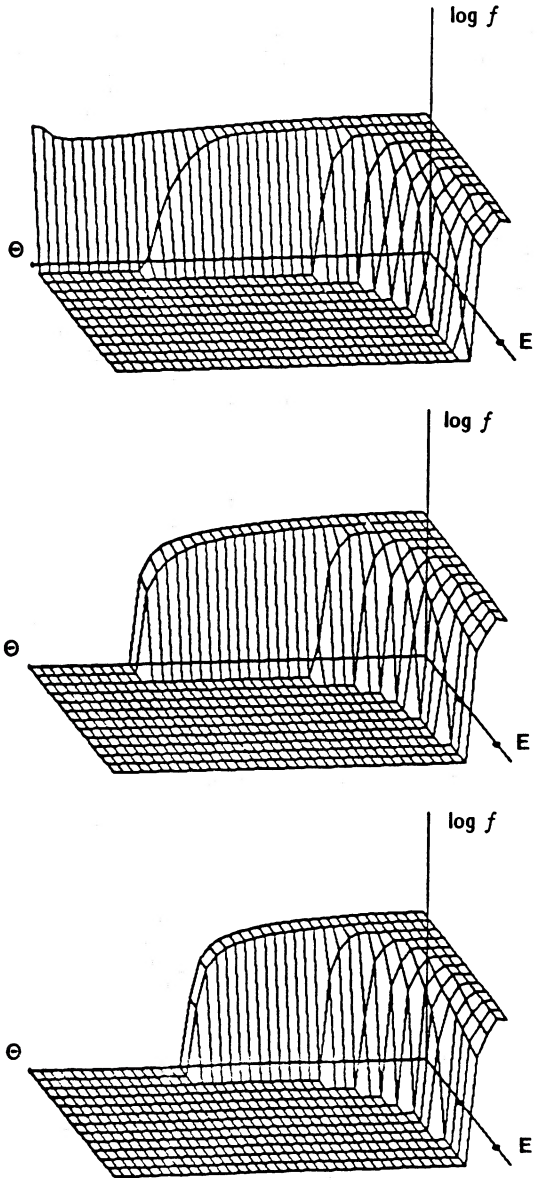

FIG. 2.—Same as Fig. 1, for $B_0 = 0.05B_c$

beam shapes become correspondingly broader. To illustrate this, the results for a half-angle of 15° and a radius of $R = 2.5$ are shown for different fields in Figure 4. It seen that the broadening is especially noticeable at low energies. This broadness is largely caused by the fact that the cutoff angles are displaced by an amount comparable to the cap half-angle. For two poles (the beams for which can be obtained from the one pole ones by reflection at 90°) this already represents a sizable fraction of the total half hemisphere. The escape profile near the axis is particularly simple at high energies near the axis, for the larger cap sizes. This is caused by the energy-dependent cutoff angle, which depends on the angle of origin within the cap. This triangular escape spike becomes more prominent as the energy and the cap opening angle is increased.

It is of interest also to investigate the dependence on the field symmetry. As an example, we considered the 1–12 MeV beam shapes for GRBs in the case when the magnetic field is assumed to be a quadrupole. We have derived the magnetic quadrupole components in the relativistic case, and used them instead of equations (6)–(10). Since the quadrupole is more complicated, the photons have a higher probability of crossing field lines at a large angle, and as a result, the beam shape of all but the lowest energies are strongly suppressed. If the emission region at the surface is taken to be again centered on the polar caps around the axis of symmetry, the escaping beam at $E \gtrsim 1$ MeV is confined to a small angular region about the axis.

V. DISCUSSION

The results of § IV show that for fields larger than a certain value $B_0 \approx 0.05B_c$ the escaping photon beam shapes do not depend significantly on further increases of the field strength. This saturation of the magnetic absorption effect is a consequence of the exponential dependence of the absorption coefficient on the field strength $B' = B/B_c$ (see eq. [3]), and this dependence is made even

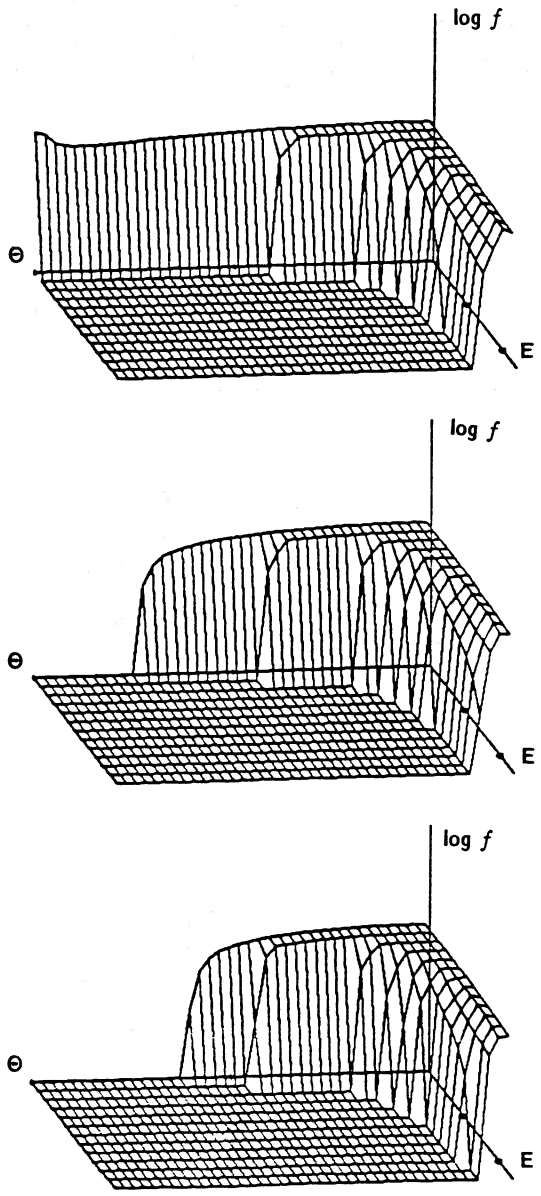

FIG. 3.—Same as Fig. 1, for $B_0 = 0.1B_c$

more sensitive by the fact that the absorption coefficient itself appears once more in an exponent, as seen in equation (16). While in the relativistic case this simple looking equation is rather involved, it is useful to look at this double exponential saturation behavior of the magnetic absorption under some approximations. This is done in Appendix B, where some simple analytic approximations are derived which describe the qualitative behavior of the solutions. We can summarize the propagation behavior of the beam as follows:

1. Photons always escape freely to an observer located in the angle range $0 \leq \Theta < \Theta_c$ (see eq. [B3]), where Θ_c is a function of the metric and of the initial photon energy. This result does not depend on the magnetic field strength.

2. For $\Theta > \Theta_c$, complete absorption occurs close to the stellar surface if the magnetic field at the surface on the polar axis B_0 satisfies

$$B_0 > 0.1B_c \, . \tag{17}$$

The observed intensity distribution is under this condition independent of magnetic field B_0. A sharp transition is obtained between a free escape and a complete absorption regime; Θ_c is then a cutoff angle.

3. For $\Theta > \Theta_c$, photon initial energy ω_0, and angle μ_0, there will be (almost) no absorption if

$$B_0 \frac{\omega_0}{m} \sqrt{1 - \mu_0^2} < 0.1B_c \; ; \tag{18}$$

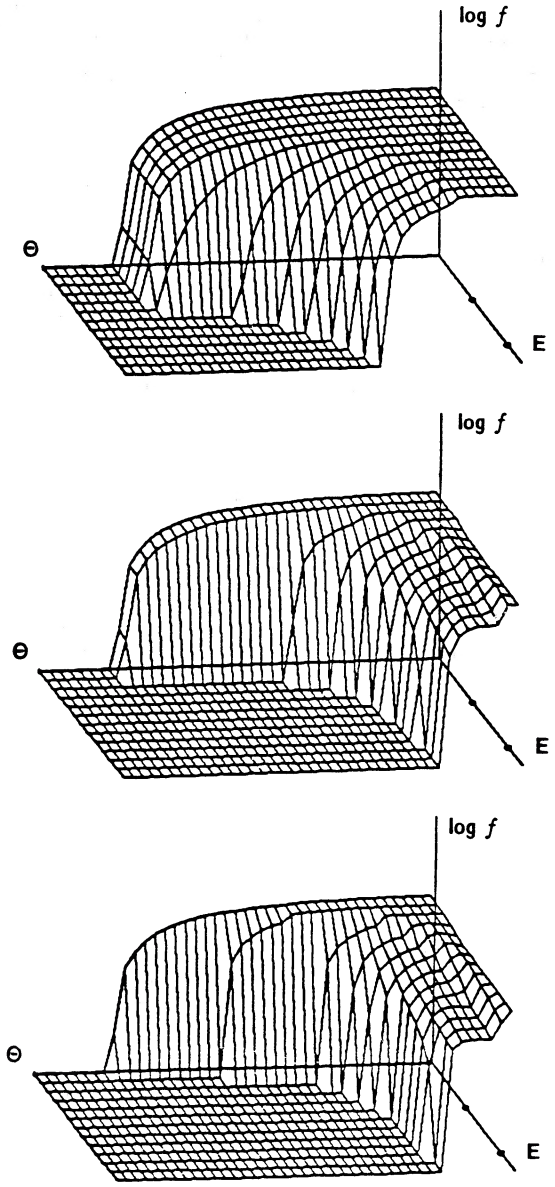

FIG. 4.—Magnetic field dependence of an $R = 2.5$, $\alpha = 15°$ one-cap configuration, for (*a*) $B_0/B_c = 0.01$, (*b*) $B_0/B_c = 0.05$, and (*c*) $B_0/B_c = 0.1$

a necessary condition for this is

$$B_0 < 0.05 B_c \, . \tag{19}$$

Equations (17)–(19) have been derived in Appendix B for the case of a beam emitted from the magnetic pole of a relativistic star. A nonrelativistic discussion has also been given by Mitrofanov *et al.* (1986). In our complete relativistic transfer calculation, however, we assumed the emission to occur from a polar cap of finite size. But if the opening angle α of the cap is small, the above approach is a reasonable approximation (the agreement with the $\alpha = 5°$ calculations is in fact quite good). For the strong field case the transition between free escape and complete absorption will then be spread over a regime of the order α around the cutoff angle. A comparison of the analytical estimates with the numerical results is most simple in the strong field case in the nonrelativistic limit, where we can identify $\mu_c \approx \cos \Theta_c$. This should be valid for the case $R = (R_*/R_S) = 5$ (see Figs. 1c, 2c, 3c). For photon energies $\hbar\omega_0 = 1., 1.5, 2.5, 5., 10.$ MeV we get from equation (B3) the cutoff angle values $\Theta_c = 72°., 42°., 24°., 12°., 6°$. Note that since in Figures 1–3 the emission occurs from caps of 5° angular size, there is a tolerance by the same amount in the values of Θ_c. Comparing these values with those in Figure 3*c* for $B_0 = 0.1 B_c$ (and also for $B_0 = B_c$), the agreement is quite good. For $B_0 = 0.1 B_c$ and $B_0 = B_c$, the quantity $ae^{-1/a}$ defined in equation (B1) is greater than 1.2×10^{-7} and 0.197, while the total optical length τ is greater than 10^4 and greater than 10^9. Thus in both cases there is complete absorption for $\Theta > \Theta_c$ and free escape otherwise, i.e., the emission pattern is essentially identical for both (and also for higher) field strengths. For $B_0 = 0.01 B_c$, the necessary condition for no absorption at some energies even at large angles is satisfied. Using equation (B6) for $\mu_0 \approx 0$, we get $\hbar\omega_0 = \omega_0' m_e c^2 \lesssim 5$ MeV in order to avoid absorption, again

in good agreement with Figure 1c. In the relativistic case, for stellar radii in Schwarzschild units $R \lesssim 4$, these values are modified by the light bending, and this effect gets stronger the smaller the radius (see Figs. 1a, 1b, 2a, 2b).

The calculations discussed here are useful in describing the high-energy characteristics of magnetic neutron star GRB models, and for testing these models against such observations as, e.g., the *SMM* statistics of the incidence of GRBs with emission above a given photon energy (Matz *et al* 1985). The present calculations can also be used for comparison with models of the emission from rotation pulsars which are detected in the MeV range. Both classes of objects are expected to become much better studied observationally in this range by the detectors on board the future GRO, Granat, and Spectrum X-ray Gamma satellites. A detailed comparison with observations would require a number of additional assumptions about the specific input spectrum and directionality, and specific model-oriented calculations, which would require a separate study. A detailed modeling of the expected detection rates of GRBs or pulsars at various energies would depend on the specific instrument characteristics, the detection criteria, and additional assumptions concerning the distribution of physical properties and the spatial densities. In the case of GRBs, this has been done by us elsewhere (Mészáros, Bagoly, and Riffert 1989).

The results of the present paper provide a fairly unencumbered and physically complete description of the essential characteristics of γ-ray–emitting relativistic magnetospheres, making a minimum of model-dependent assumptions. There are a number of relevant conclusions which emerge from these relatively assumption-free simple models. One can see from the beam shapes of Figures 1–4 that the general relativistic effects can have a significant impact on the detection probability by broadening the escaping beam in the more compact stellar configurations. In fact, the detectability of high-energy photons ($\gtrsim 5$ MeV) is significantly greater than one would derive from a flat space mean free path argument using the cross section of equation (3a). The less massive neutron stars, which for a standard equation of state are expected to have a smaller radius in Schwarzschild units, should be easier to detect at high energies than the higher mass ones. A very interesting result is that for $B_0 \gtrsim 0.05 B_c$, the escaping high-energy photon beams do not depend on the field strength. Since for $B_0 = 0.05 B_c$ the beam shapes are still of reasonable angular size, there should be a fair probability of detecting high-energy emission ($E \gtrsim 10$ MeV) even from high field neutron stars ($B_0/B_c \gtrsim 0.1$–1), if such photons are produced and are not absorbed by some process other than magnetic absorption.

We are grateful to A. Harding for her suggestions. This research has been supported in part through NSF grants AST 85–14735 at Penn State and NSF 83–51997, NASA Astrophysical Theory Center Grant NAGW–766, and grants from Ball Aerospace Systems Division, Rockwell International Corporation, and Exxon Education Foundation at JILA.

APPENDIX A

RADIATIVE TRANSFER

The radiative transfer equation (15) can be written in a Schwarzchild metric [with coordinates (t, r, Θ, Φ)], assuming rotational symmetry ($\partial/\partial\Phi = 0$) and stationarity ($\partial/\partial t = 0$) as follows (Riffert 1986; Riffert and Mészáros 1988)

$$A\mu \frac{\partial f}{\partial r} + \frac{\sqrt{1-\mu^2}}{r}\left(\cos\phi \frac{\partial f}{\partial \Theta} - \sin\phi \cot\Theta \frac{\partial f}{\partial \phi}\right) + \frac{1-\mu^2}{r}\left(A - r\frac{dA}{dr}\right)\frac{\partial f}{\partial \mu} - \frac{dA}{dr}\mu\omega \frac{\partial f}{\partial \omega} = -\kappa_A R_S f , \tag{A1}$$

where f is the invariant photon distribution function, ω is the photon energy, μ is the cosine of the angle between the radial direction and the photon momentum, and ϕ is the corresponding azimuthal angle. The radius r is measured in units of the Schwarzschild radius $R_S = 2GM/c^2$ and $A = [1 - (1/r)]^{1/2}$. The absorption coefficient κ_A is discussed in § II; it contains a dependence of the magnetic field and of the photon four-momentum. Thus it is a function of all the variables

$$\kappa_A = \kappa_A(r, \Theta, \mu, \phi, \omega) .$$

The transfer equation (A1) can be solved by the methods of characteristics (see Riffert and Mészáros 1988, for the vacuum case), and the boundary conditions are specified on the stellar surface; i.e., we assume a given distribution $f = f_0$ at $r = R$. Then, for an observer at large distances ($r_{obs} \gg R$), the solution can be written as

$$f = f_0 e^{-\tau} ,$$

where τ is the total optical depth along the photon path:

$$\tau = R_* \int_0^1 \frac{\kappa_A(r/z, \Theta_z, \mu_z, \omega_z)}{z^2 \mu_z \sqrt{1 - z/r}}\, dz \tag{A2}$$

($R_* = RR_S$ is the stellar radius in cm). The variable z parameterizes the photon path from the stellar surface ($z = 1$) to infinity ($z = 0$), and from the characteristics of equation (1) we have:

$$\mu_z = \left[1 - u^2\left(1 - \frac{z}{r}\right)z^2\right]^{1/2}, \quad \omega_z = \omega_0\left(\frac{1 - 1/r}{1 - z/r}\right)^{1/2}, \quad \cos\Theta_z = \cos\Theta\cos K_z + \cos\phi \sin\Theta \sin K_z , \tag{A3}$$

$$\sin\phi_z = \frac{\sin\Theta \sin\phi}{\sin\Theta_z}, \quad K_z = u\int_0^z \left[1 - u^2\left(1 - \frac{t}{r}\right)t^2\right]^{-1/2} dt , \quad u = \left(\frac{1-\mu_0^2}{1 - 1/r}\right)^{1/2} .$$

The relations (A3) contain a number of integration constants from the characteristic equations: the observer's coordinates are (r_{obs}, Θ), and the photons arrive there with a three-momentum

$$\boldsymbol{k} = \omega(\mu, \sqrt{1-\mu^2}\cos\phi, \sqrt{1-\mu^2}\sin\phi)\,,$$

where

$$\mu = \sqrt{1 - u^2\frac{R^2}{r_{obs}^2}}\,, \qquad \omega = \omega_0\sqrt{1-\frac{1}{R}}\,.$$

These photons have been emitted from the stellar surface with the frequency ω_0 in a direction given by (μ_0, ϕ_0). The relation between the emission and the observation parameters can be easily obtained from equation (A3) taking the limits $z = 1$ and $z = 0$.

The observationally relevant quantity is the radial flux component at large distances:

$$F = \omega^3 \iint_{4\pi} f\mu\, d\mu\, d\phi = 2\omega_0^3\left(\frac{R}{r_{obs}}\right)^2\sqrt{1-\frac{1}{R}}\iint_{S_0} f_0(\Theta, \mu_0, \omega_0)e^{-\tau}\mu_0\, d\mu_0\, d\phi\,.$$

We have used here the characteristics of equation (A1) to express the solid angle integral at the observer's location in terms of the emission quantity μ_0. However, for practical reasons we retain the variable ϕ (instead of ϕ_0); S_0 stands for the part of the μ_0-ϕ-regime, where $f_0 \neq 0$, and it is a subset of the rectangle $(0 \le \mu_0 \le 1, 0 \le \phi \le \pi)$. For the case that the emission is confined to a fraction of the stellar surface around the pole given by the (half) opening angle α, the ϕ-integration is limited by $0 \le \phi \le \phi_L$, where

$$\phi_L = \begin{cases} \arccos\Psi, & -1 \le \Psi \le 1, \\ 0, & \Psi > 1, \\ \pi, & \Psi < -1, \end{cases}$$

and

$$\Psi = \frac{\cos\alpha - \cos\Theta\cos K}{\sin\Theta\sin K}\,,$$

with $K = K_z(z = 1)$(see also Riffert and Mészáros 1988).

APPENDIX B

PHOTON PROPAGATION

In this Appendix we derive some simple relations in order to describe the propagation and absorption behavior of a photon beam in the magnetic field of the neutron star. Although we restrict ourselves to a special case, the results show some general aspects of the complete transfer problem described in § IV of this paper. For a beam of photons emitted from the stellar surface at the pole of a dipole magnetic field, the photon path is characterized by (see Appendix A):

$$\sin\phi_z = 0\,, \qquad \cos\Theta_z = \cos\hat{K}_z\,, \qquad \hat{K} = u\int_z^1 [1 - u^2(1 - t/R)t^2]^{-1/2}\,dt$$

(u and the remaining variables μ_z and ω_z are defined in equation [A3]).

We now estimate the optical length τ (eq. [A2]) for this beam. For simplicity the following expression for the absorption coefficient will be used:

$$\kappa_A = \begin{cases} 4.347\times 10^7\dfrac{B}{B_c}\sin\lambda\exp\left(-\dfrac{4}{3\chi}\right), & \text{if } \dfrac{\omega}{2m}\sin\lambda > 1\,, \\ 0 & \text{otherwise}\,, \end{cases}$$

where

$$\chi = \frac{\omega}{2m}\frac{B}{B_c}\sin\lambda(z)\,,$$

and $\lambda(z)$ is the local angle between the magnetic field and the beam direction. This expression is a reasonable approximation, not too close to the threshold energy. We rewrite the optical length integral as

$$\tau = b\int_\Sigma \frac{z}{\mu_z}Q(z)\exp\left[-\frac{1}{az^3Q(z)}\right]dz\,, \tag{B1}$$

where

$$a = \frac{3\omega_0}{8m}\frac{B_0}{B_c}\sqrt{1-\mu_0^2}\,, \qquad b = 4.347\times 10^7 R_*\frac{B_0}{B_c}\sqrt{1-\mu_0^2}\,,$$

and B_0 is the surface field defined in equation (8). The photons are emitted with frequency ω_0 and an angle arccos μ_0 respect to the polar axis. The set Σ defines those parts of the z-integration interval for which $\kappa_A \neq 0$; i.e.,

$$\Sigma = \left\{ z \left| \frac{\omega_z}{2m} \sin\lambda(z) > 1;\ 0 \le z \le 1 \right.\right\}.$$

The function $Q(z)$ contains the details of the field geometry and the local propagation direction; for a dipole magnetic field,

$$Q(z) = \frac{1}{\mathscr{F}_1(R)}\left| \mathscr{F}_1\left(\frac{R}{z}\right) z\cos\hat{K}_z - \frac{1}{2}\mathscr{F}_2\left(\frac{R}{z}\right)\left(\frac{1}{u}\sin\hat{K}_z\right)\sqrt{\left(1-\frac{z}{R}\right)^{-1} - u^2z^2}\right|$$

[note that for $u \to 0$ (or $\mu_0 \to 1$) $\sin(\hat{K}_z)/u = 1 - z + O(u^2)$].

The kinematic relation appearing in the definition of Σ can be written as

$$\Psi(z) \equiv \frac{\omega_0}{2m}\sqrt{1-\mu_0^2}\,\Omega(z) > 1\,,$$

where

$$\Omega = \frac{|z\cos\hat{K}_z - g[(1/u)\sin\hat{K}_z]\sqrt{(1-z/R)^{-1} - u^2z^2}|}{\cos^2\hat{K}_z + g^2\sin^2\hat{K}_z}\,,$$

and

$$g = \frac{\mathscr{F}_1(R/z)}{2\mathscr{F}_2(R/z)}\,.$$

It can be shown that $\Omega \le 1$ holds for all R, $\mu_0 \ge 0$; thus, if the photons are emitted in the range of angles

$$\mu_c < \mu_0 \le 1, \text{ where } \mu_c = \sqrt{1-\left(\frac{2m}{\omega_0}\right)^2}\,, \tag{B2}$$

one has $\Psi(z) < 1$, and there will be no absorption at all because the kinematic condition is not fulfilled anywhere along the photon path. Photons emitted under $\mu_0 = \mu_c$ travel to an observer located at $\Theta = \Theta_c$, where

$$\Theta_c = u_c\int_0^1 [1 - u_c^2(1-t/R)t^2]^{-1/2}\,dt\,, \tag{B3}$$

and

$$u_c = \frac{2m}{\omega_0}\left(1-\frac{1}{R}\right)^{-1/2}.$$

Assuming $\Theta_c \le \pi$ (which holds for $\omega_0/2m > 1.01$ and $R > 1.58$), the relation between μ_0 and μ_c can be transformed in a simple way into one for Θ and Θ_c. At large distances from the star the beam will be observable for

$$0 \le \Theta < \Theta_c\,.$$

For the emission regime $\mu_0 < \mu_c$ the kinematic relation defines a set of integration intervals for the optical length integral. However, there is always one of those intervals close to $z = 1$, because $\Omega(1) = 1$; i.e., for $\mu_0 < \mu_c$ some absorption occurs close to the stellar surface. This regime gives the main contribution to the integral (B1) because of the factor

$$\exp\left[-\frac{1}{az^3Q(z)}\right].$$

We therefore write for the optical depth

$$\tau = be^{-1/a}\Gamma(\mu_0, R, \omega_0, B_0)\,,$$

where

$$\Gamma = \int_\Sigma \frac{z}{\mu_z}Q(z)\exp\left\{-\frac{1}{a}\left[\frac{1}{z^3Q(z)} - 1\right]\right\}dz\,,$$

and, if μ_0 is not too close to μ_c (where $\Gamma = 0$), then Γ depends only weakly on the parameters μ_0, R, ω_0, B_0.

In the regime we are interested in, i.e., $10^{-2} < B_0 < 10$, $2 < \omega_0/m < 10^3$, $R > 1.5$, Γ varies between 0.01 and 0.5 (this can be shown by a detailed numerical study of Γ). From the definition of the constant b we get

$$\tau \approx 3.5 \times 10^{13} \Gamma \frac{M}{M_\odot} \frac{R_*}{R_S} \frac{mc^2}{h\omega_0} a e^{-1/a} . \tag{B4}$$

The depth τ will be of the order of unity only for small values of a, where the function $a \exp(-1/a)$ is extremely steep (for $0.03 < a < 0.07$ it varies between 10^{-16} and 4.0×10^{-8}). For $\mu_0 < \mu_c$, we have $a > 3B_0/4B_c$, and thus

$$\tau \gg 1 , \qquad \text{if} \quad \frac{B_0}{B_c} > 0.1 . \tag{B5}$$

All photons will be absorbed then. In order to avoid complete absorption the parameter a has to be typically $a < 0.04$ (independent of ω_0), and we get

$$\frac{B_0}{B_c} \frac{\omega_0}{m} \sqrt{1 - \mu_0^2} < 0.1 . \tag{B6}$$

From the kinematic relation $\omega_0/m(1 - \mu_0^2)^{1/2} > 2$, therefore,

$$\frac{B_0}{B_c} < 0.05 \tag{B7}$$

is a necessary condition for the photons to escape from the emission regime $\mu_0 < \mu_c$.

REFERENCES

Brainerd, J. J. 1989, *Ap. J.*, in press.
Daugherty, J. K., and Bussard, R. W. 1980, *Ap. J.*, **238**, 296.
Daugherty, J. K., and Harding, A. K. 1983, *Ap. J.*, **273**, 761.
Harding, A. K. 1986, *Ap. J.*, **300**, 167.
Lamb, D. Q. 1988, in *AIP Conf. Proc. Nuclear Spectoscopy of Astrophysical Sources*, ed. N. Gehrels and G. Share (New York: AIP), in press.
Matz, S. M., *et al.* 1985, *Ap. J. (Letters)*, **288**, L37.
Mazets, E. P., *et al.* 1981, *Nature*, **290**, 378.
Mészáros, P., Bagoly, Z., and Riffert, H. 1989, *Ap. J. (Letters)*, **337**, L23.
Mészáros, P., and Riffert, H. 1987, *Ap. J. (Letters)*, **323**, L127.
Mitrofanov, I. G., *et al.* 1986, *Soviet Astr.*, **30**, 659.
Murakami, T., *et al.* 1988, *Nature*, **335**, 234.
Riffert, H. 1986. *Ap. J.*, **310**, 729.
Riffert, H., and Mészáros, P. 1988, *Ap. J.*, **327**, 712.
Rybicki, G. B., and Lightman, A. P. 1979, *Radiative Processes in Astrophysics* (New York: Wiley).
Trümper, J. 1987, in *Very High Energy Gamma Rays in Astronomy*, NATO ASI Ser., Vol. **199**, ed. K. Turver (Dordrecht: Reidel), p. 7.
Tsai, W., and Erber, T. 1974, *Phys. Rev. D*, **10**, 492.
Wasserman, I. M., and Shapiro, S. L. 1983, *Ap. J.*, **265**, 1036.
Zdziarski, A. 1987, in *Proc. 13th Texas Symposium Relativistic Astrophysics*, ed. M. Ulmer (Singapore: World Scientific), p. 563.

Z. BAGOLY AND P. MÉSZÁROS: 525 Davey Lab, Pennsylvania State University Park, PA 16802

H. RIFFERT: JILA, University of Colorado, Box 440, Boulder, CO 80309